MdNup62 interactions with MdHSFs involved in flowering and heat-stress tolerance in apple

Chenguang Zhang†, Na An†, Pen Jia†, Wei Zhang, Jiayan Liang, Hua Zhou, Dong Zhang, Juanjuan Ma, Caiping Zhao, Mingyu Han, Xiaolin Ren, Libo Xing*

[1]College of Horticulture, Northwest A&F University, 712100 Yangling, Shaanxi, P. R. China

†Equal contributors

***Corresponding author:**

Libo Xing

E-mail: libo_xing@nwsuaf.edu.cn ;

Tel.: +8615129227289;

ORCID: https://orcid.org/0000-0002-8918-7128;

Address: 3 Taicheng Road, Yangling 712100, Shaanxi, P. R. Chin

Run title: MdNup62 interactions with MdHSFs regulate flowering and heat-stress tolerance

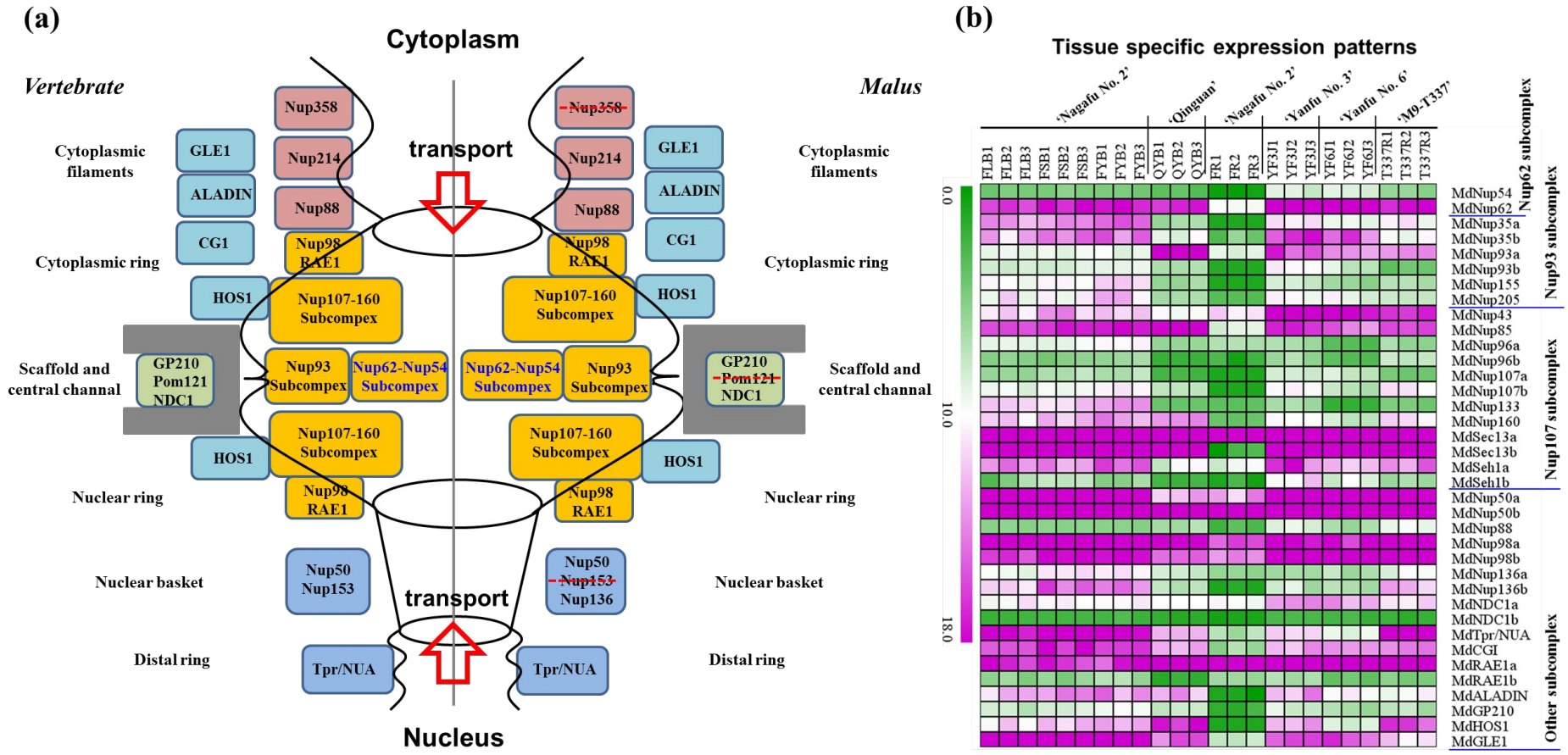

Figure 1. The nuclear pore complex (NPC) structure and composition in *Vertebrate* and *Malus*.
(a) A schematic of the nuclear pore with the cytoplasmic side at the top and the nuclear basket at the bottom for Vertebrate (left) and Malus (right). (b) Tissue specific expression patterns of apple NPC components by RNA-seq. The full names of the different abbreviations are as follows, 'Nagafu No.2' long branches flower buds (FLB), 'Nagafu No.2' short branches flower buds (FSB), 'Nagafu No.2' axillary buds (FYB), 'Qinguan' axillary buds (QYB), 'Nagafu No.2' fruit (FR), 'Yanfu No.3' stem tip (YF3J), 'Yanfu No.6' stem tip (YF6J), and 'M9-T337' root (T337R). Each number after the abbreviation represents a biological repetition.

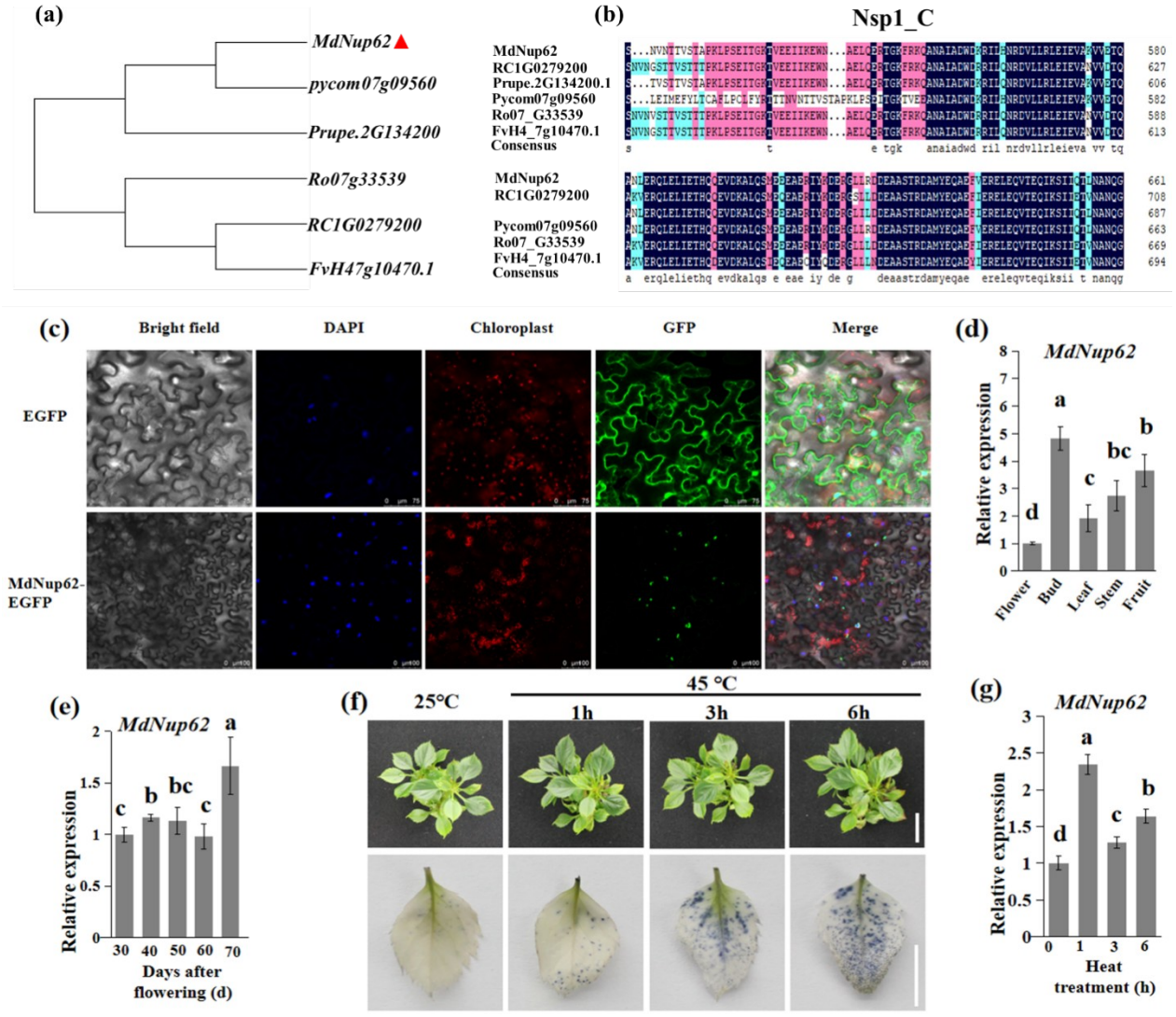

Figure 2. Identification and analysis of *MdNup62*.

(a) Phylogenetic analysis of Rosaceae *Nup62*. (b) The conservative domain of Rosaceae *Nup62*. (c) Subcellular localization of *MdNup62*. The upper panel shows 35S::EGFP, and the lower panel shows 35S::MdNup62-EGFP. (d) and (e) Analyses of *MdNup62* expression levels in diverse 'Nagafu No. 2' apple tissues (d) and in different flower bud developmental stages of 'Nagafu No. 2' (e). (f) The phenotype of 'Nagafu No. 2' tissue-cultured seedlings (upper panels) and the in situ accumulation of superoxide radical (O^{2-}) at 0, 1, 3, and 6 h under heat treatment conditions (lower panels). Bar = 1 cm. (g) *MdNup62* expression levels in 'Nagafu No. 2' tissue-cultured seedling leaves at 0, 1, 3, and 6 h under heat-treatment conditions. Each sample was analysed with three biological replicates, each comprising three technical replicates. Means followed by different lowercase letters are significantly different at the 0.05 level.

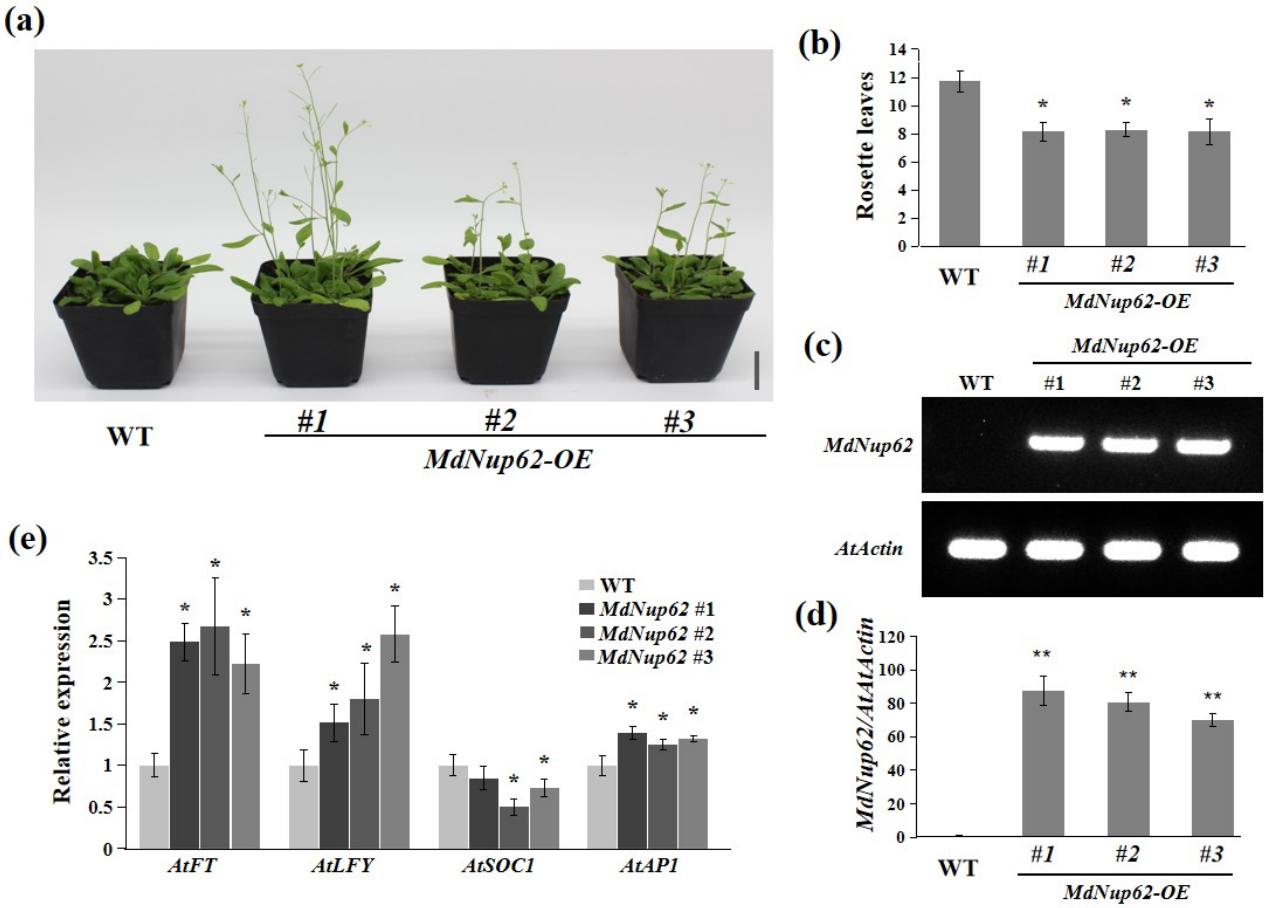

Figure 3

Figure 3. *MdNUP62* promotes flowering in Arabidopsis.
(a) Phenotype of the *MdNUP62*-overexpression Arabidopsis line for flowering time. Bar = 2 cm. (b) Statistical analysis of rosette leaves of *Arabidopsis thaliana* during bolting. Asterisks denote significant differences as determined by a t-test (*P < 0.05). (c) Semi-quantitative RT-PCR analysis of *MdNup62* expression in Arabidopsis samples. (d) qRT-PCR analysis of *MdNup62* expression in Arabidopsis samples. Asterisks denote significant differences as determined by a t-test (*P < 0.01). (e) Relative expression levels of flowering genes (*AtFT*, *AtLFY*, *AtSOC1*, and *AtAP1*) in WT and *MdNup62*-overexpression lines. Each sample was analysed with three biological replicates, each comprising three technical replicates. Asterisks denote significant differences as determined by a t-test (*P < 0.05).

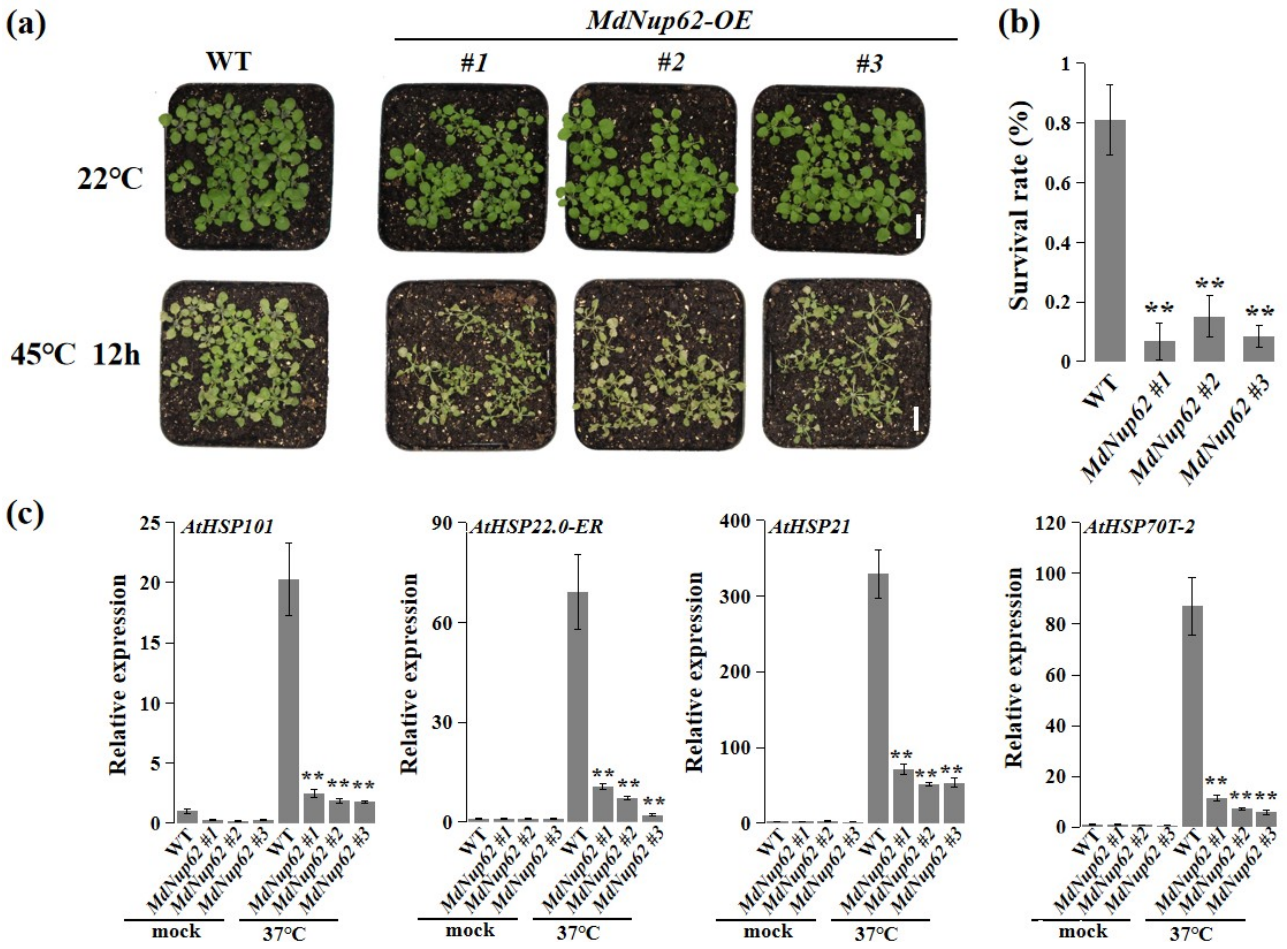

Figure 4. *MdNup62* reduced high-temperature resistance in Arabidopsis.
(a) Phenotype of the *MdNup62*-overexpression Arabidopsis line for high-temperature resistance. Bar = 1cm. (b) Survival rates of WT and *MdNup62*-overexpression Arabidopsis lines after the high-temperature treatment. Asterisks denote significant differences as determined by a t-test (**P < 0.01). (c) Relative expression levels of high-temperature resistance-related genes (*AtHSP101*, *AtHSP22.0-ER*, *AtHSP21*, and *AtHSP70T-2*) in WT and *MdNup62*-overexpression lines at the normal (22°C) temperature and 1 h after exposure to the high-temperature (37°C) treatment. Each sample was analysed with three biological replicates, each comprising three technical replicates. Asterisks denote significant differences as determined by a t-test (**P < 0.01).

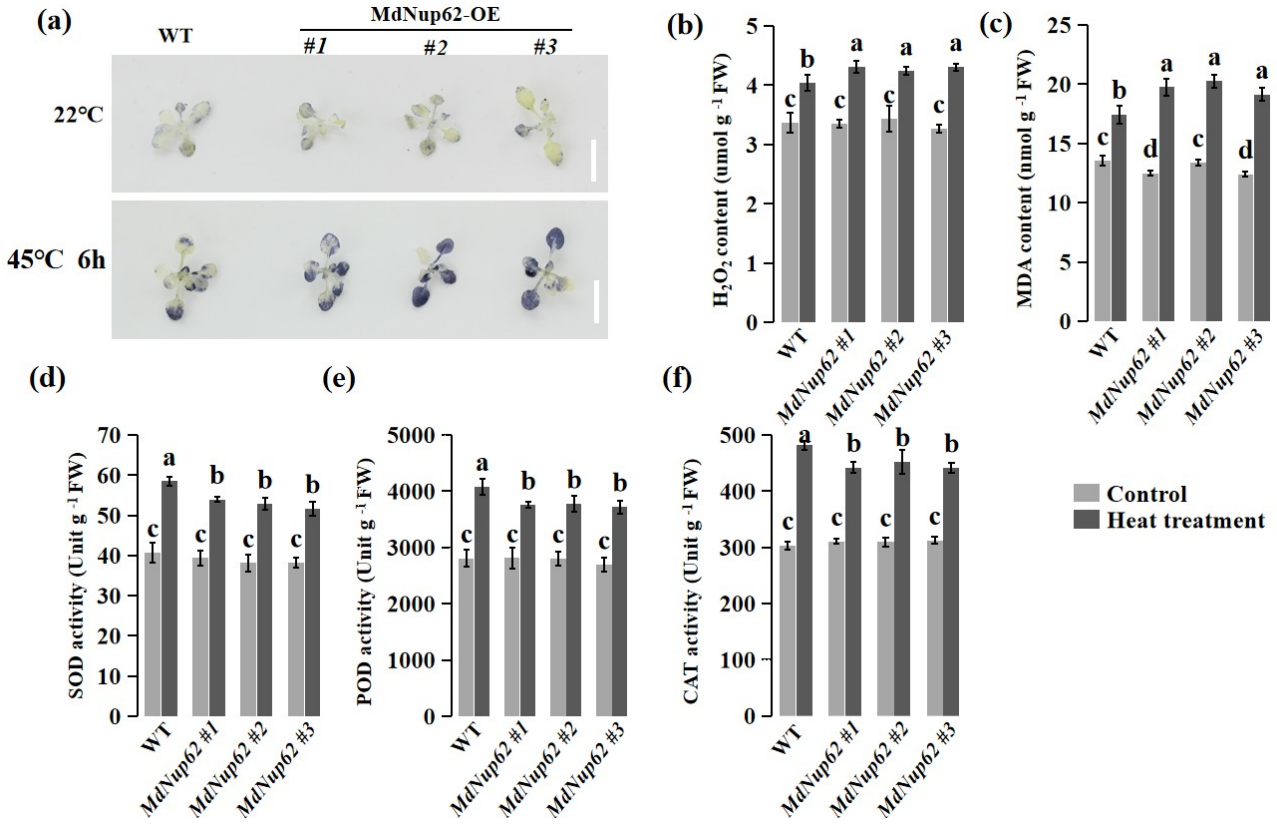

Figure 5. Changes in the level of accumulated ROS and activities of ROS-scavenging enzymes in *OE-MdNup62* and WT Arabidopsis leaves under heat-stress conditions.

(a) In situ accumulations of superoxide radicals (O^{2-}) before (upper panels) and after (lower panels) heat treatment as revealed by nitro blue tetrazolium staining. (b) and (c) Quantitative measurement of H_2O_2 and malondialdehyde concentrations in Arabidopsis leaves treated with and without the high temperature. (d)–(f) Activities of superoxide dismutase (SOD), peroxidase (POD), and catalase (CAT) at 6 h after the heat treatment. Each sample was analysed with three biological replicates, each comprising three technical replicates. Means followed by different lowercase letters are significantly different at the 0.05 level.

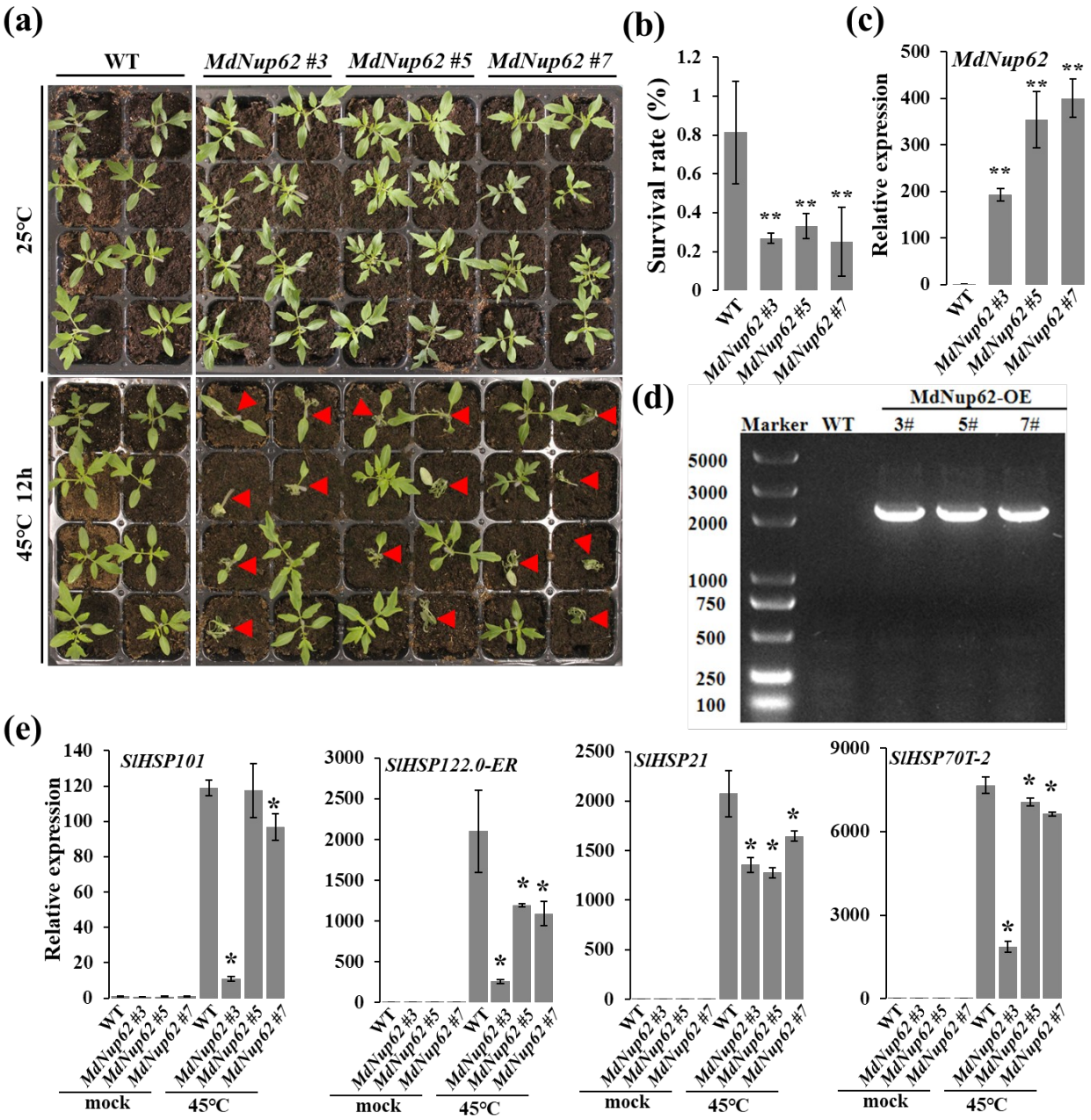

Figure 6. *MdNup62* reduced high-temperature resistance in tomato.
(a) Phenotype of the *MdNup62*-overexpression tomato line for high-temperature resistance. Bar = 5 cm. (b) Survival rates of WT and *MdNup62*-overexpression tomato lines after the high-temperature treatment. Asterisks denote significant differences as determined by a t-test (**P < 0.01). (c) qRT-PCR analysis of *MdNup62* expression levels in tomato samples. Asterisks denote significant differences as determined by a t-test (**P < 0.01). (d) Genomic PCR analysis of *MdNup62* transgenic tomato lines. (e) Relative expression levels of high-temperature resistance-related genes (*SlHSP101*, *SlHSP22.0-ER*, *SlHSP21*, and *SlHSP70T-2*) in WT and *MdNup62*-overexpression lines at the normal temperature (22°C) and 1 h after exposure to the high-temperature (45°C) treatment. Each sample was analysed with three biological replicates, each comprising three technical replicates. Asterisks denote significant differences as determined by a t-test (*P < 0.05).

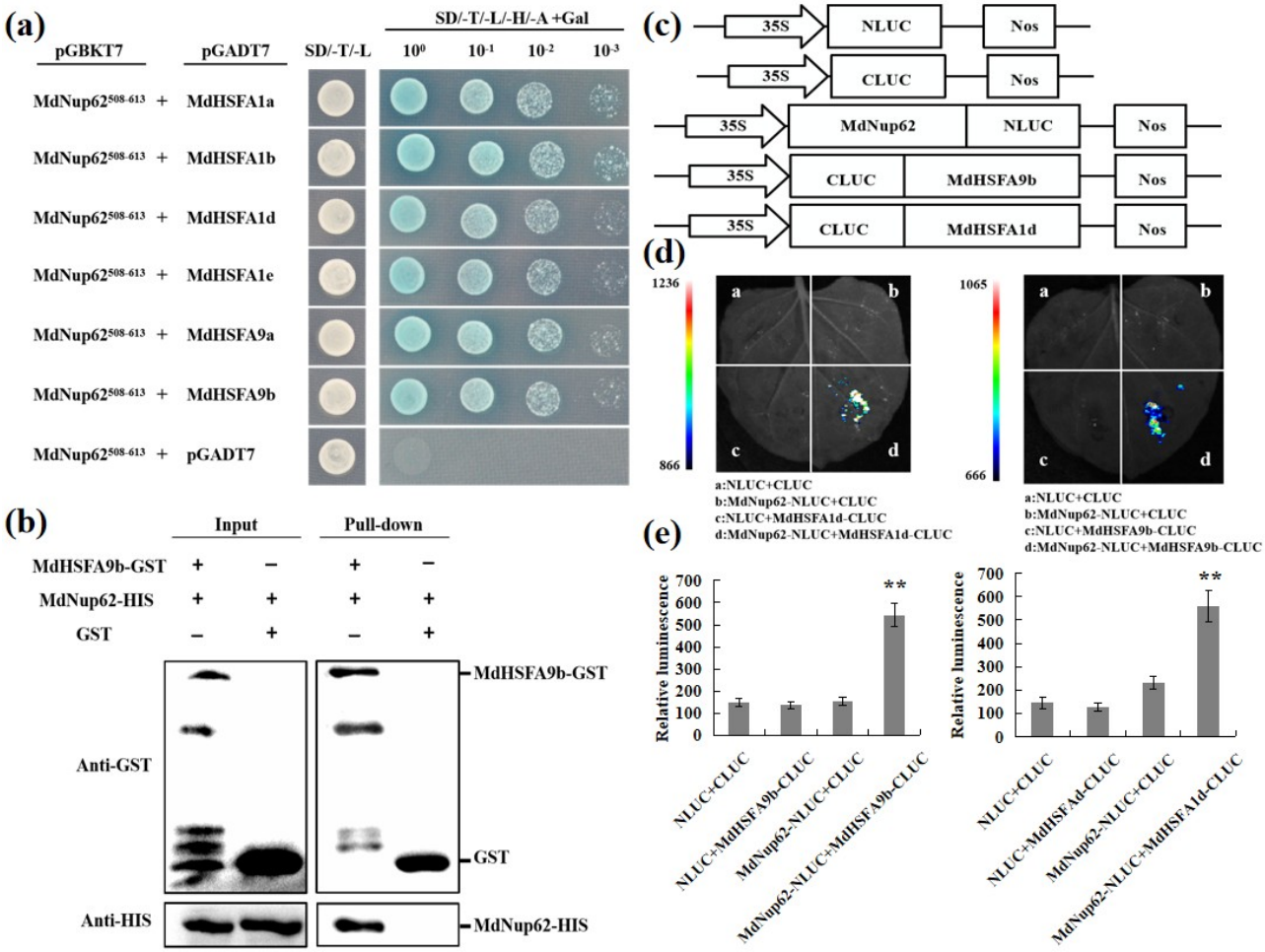

Figure 7. *MdNup62* interacts with *MdHSF*s.

(a) Interactions between *MdNup62*$^{508-613}$ and *MdHSF*s (*MdHSFA9a/b* and *MdHSFA1a/b/d/e*) in Y2H assays. The *MdNup62*$^{508-613}$ truncated sequence was cloned into pGBKT7, whereas *MdHSFA*s (*MdHSFA9a/b* and *MdHSFA1a/b/d/e*) were cloned independently into the pGADT7 vector. Empty pGADT7 plus *MdNup62*$^{508-613}$-pGBKT7 was used as the control. (b) Interactions between *MdNup62* and *MdHSFA9b* in the pull-down assay. Western blotting with a GST antibody revealed that *MdNup62-HIS* was pulled down by *MdHSFA9b-GST*. (c)–(e) Interactions between *MdNup62* and both *MdHSFA9b* and *MdHSFA1d* in a luciferase (LUC) complementation experiment. Empty NLUC and empty CLUC, *MdNup62*-NLUC plus empty CLUC, empty NLUC plus *MdHSFA9b*, and *MdHSFA1d*-CLUC were used as controls. The LUC complementation experiment was repeated three times, with consistent results. Asterisks denote significant differences as determined by t-tests (** $P < 0.01$).

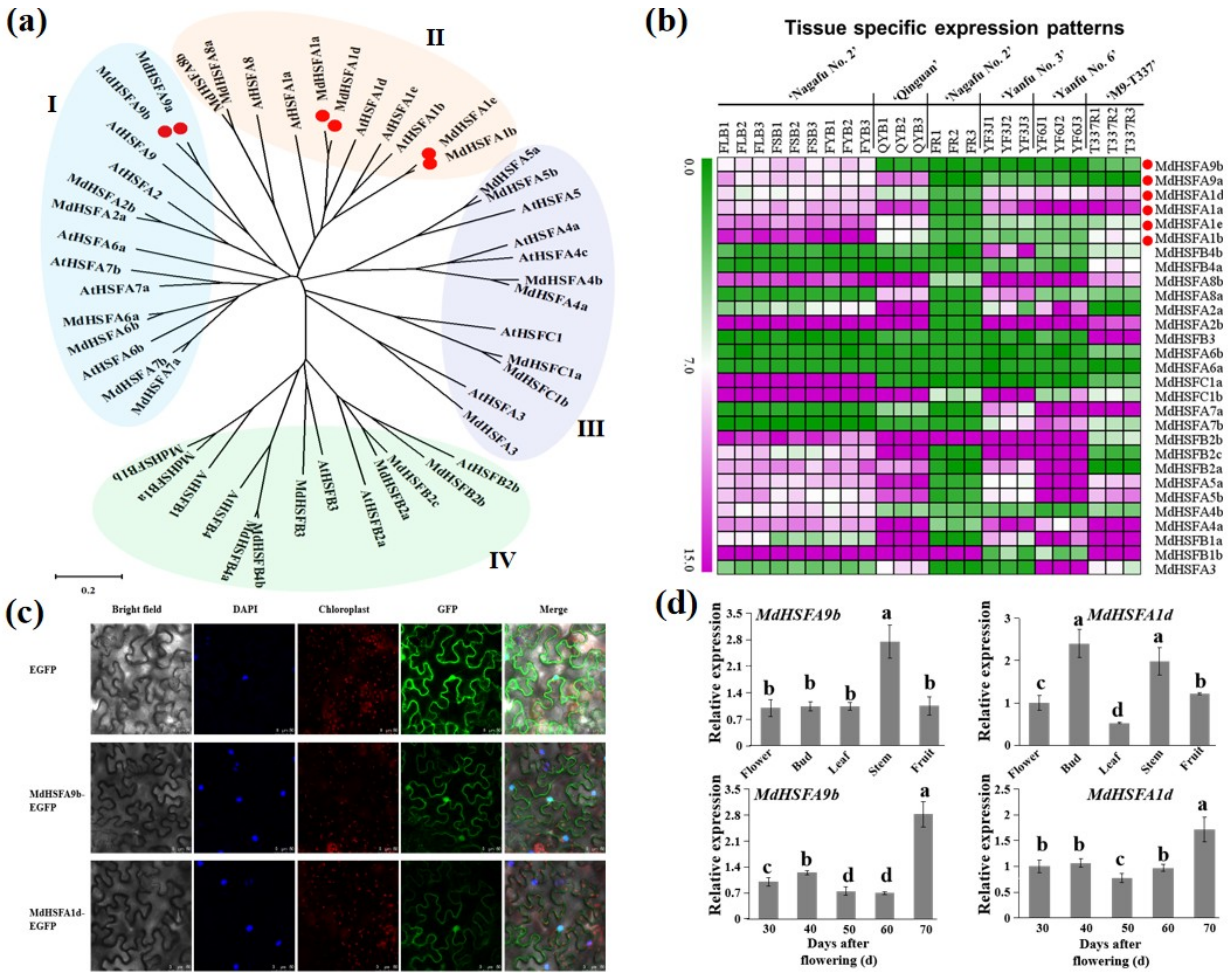

Figure 8. Subcellular localization and expression analyses of *MdHSFA9b* and *MdHSFA1d.*

(a) Phylogenetic analysis of *HSFs* in Malus and Arabidopsis.(b) Tissue specific expression patterns of apple *MdHSFs* by RNA-seq. The full names of the different abbreviations are as follows, 'Nagafu No.2' long branches flower buds (FLB), 'Nagafu No.2' short branches flower buds (FSB), 'Nagafu No.2' axillary buds (FYB), 'Qinguan' axillary buds (QYB), 'Nagafu No.2' fruit (FR), 'Yanfu No.3' stem tip (YF3J), 'Yanfu No.6' stem tip (YF6J), and 'M9-T337' root (T337R). Each number after the abbreviation represents a biological repetition. (c) Subcellular localizations of *MdHSFA9b* and *MdHSFA1d*. The upper panel shows 35S::EGFP, the middle panel shows 35S::*MdHSFA9b*-EGFP, and the lower panel shows 35S::*MdHSFA1d*-EGFP. (d) Analyses of *MdHSFA9b* and *MdHSFA1d* expression levels in diverse apple 'Nagafu No. 2' tissues and in different flower bud developmental stages of 'Nagafu No. 2'. Each sample was analysed with three biological replicates, each comprising three technical replicates. Means followed by different lowercase letters are significantly different at the 0.05 level.

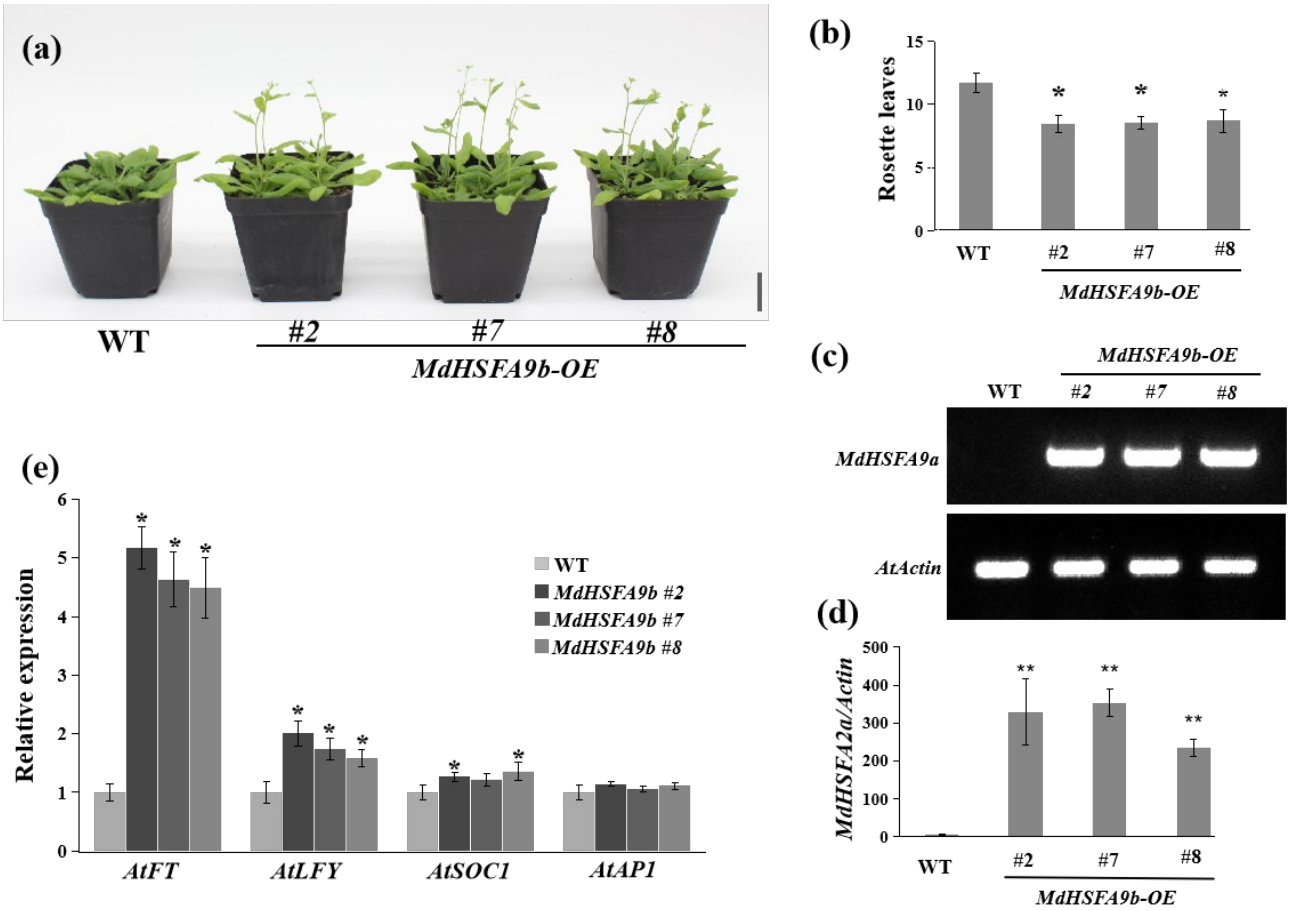

Figure 9. *MdHSFA9b* promotes flowering in Arabidopsis.

(a) Phenotype of the *MdHSFA9b*-overexpression Arabidopsis line for flowering time. Bar = 2 cm. (b) Statistical analysis of rosette leaves of *Arabidopsis thaliana* during bolting. Asterisks denote significant differences as determined by a t-test (*P < 0.05). (c) Semi-quantitative RT-PCR analysis of *MdHSFA9b* expression in Arabidopsis samples. (d) qRT-PCR analysis of *MdHSFA9b* expression in Arabidopsis samples. Asterisks denote significant differences as determined by a t-test (**P < 0.01). (e) Relative expression levels of flowering genes (*AtFT*, *AtLFY*, *AtSOC1*, and *AtAP1*) in WT and *MdHSFA9b*-overexpression lines. Each sample was analysed with three biological replicates, each comprising three technical replicates. Asterisks denote significant differences as determined by a t-test (*P < 0.05).

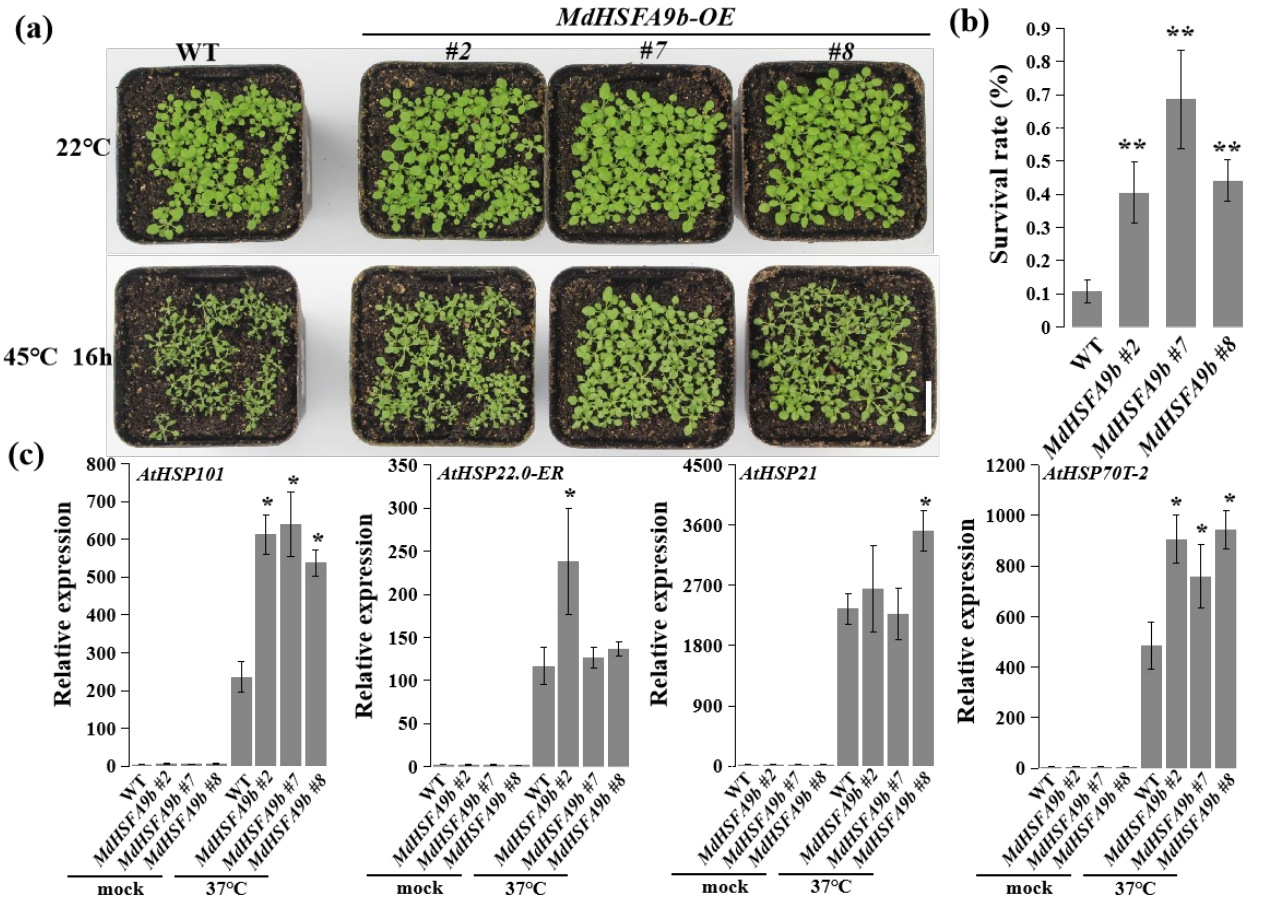

Figure 10. *MdHSFA9b* enhanced high-temperature resistance in Arabidopsis. (a) Phenotype of the *MdHSFA9b*-overexpression Arabidopsis line for high-temperature resistance. Bar = 2 cm. (b) Survival rates of WT and *MdHSFA9b*-overexpression Arabidopsis lines after the high-temperature treatment. Asterisks denote significant differences as determined by a t-test (**P < 0.01). (c) Relative expression levels of high-temperature resistance-related genes (*AtHSP101*, *AtHSP22.0-ER*, *AtHSP21*, and *AtHSP70T-2*) in WT and *MdHSFA9b*-overexpression lines at the normal temperature (22°C) and 1 h after exposure to the high-temperature (45°C) treatment. Each sample was analysed with three biological replicates, each comprising three technical replicates. Asterisks denote significant differences as determined by a t-test (*P < 0.05).

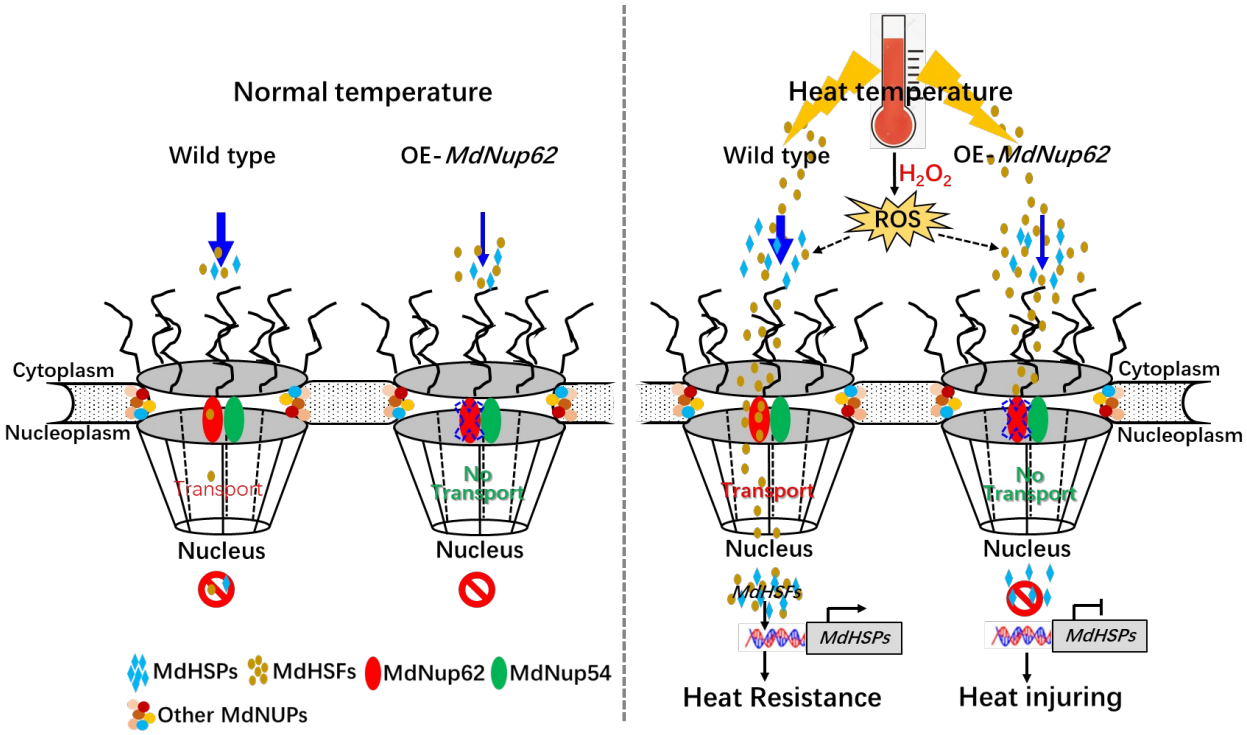

Figure 11. Model of MdNup62 interactions with MdHSFs involved in flowering and heat-stress tolerance in apple.